S. pombe btn1, the orthologue of the Batten disease gene *CLN3*, is required for vacuole protein sorting of Cpy1p and Golgi exit of Vps10p

Sandra Codlin[1] and Sara E. Mole[1,2,3,*]

[1]MRC Laboratory for Molecular Cell Biology, [2]Molecular Medicine Unit, UCL Institute of Child Health and [3]Department of Genetics, Evolution and Environment, University College London, London WC1E 6BT, UK

*Author for correspondence (e-mail: s.mole@ucl.ac.uk)

Accepted 16 December 2008
Journal of Cell Science 122, 1163-1173 Published by The Company of Biologists 2009
doi:10.1242/jcs.038323

Summary

Batten disease is characterised by lysosomal dysfunction. The most common type of the disease is caused by mutations in the membrane protein CLN3, whose function is unknown. We show that the fission yeast orthologue Btn1p, previously implicated in vacuole function, is required for correct sorting of the vacuole hydrolase carboxypeptidase Y (Cpy1p). This is, in part, due to a defect in trafficking of Vps10p, the sorting receptor for Cpy1p, from the Golgi to the *trans*-Golgi network in *btn1*Δ cells. Our data also implicate *btn1* in other Vps10-independent Cpy1-sorting pathways. Furthermore, *btn1* affects the number, intracellular location and structure of Golgi compartments. We show that the prevacuole location of Btn1p is at the Golgi, because Btn1p colocalises predominantly with the Golgi marker Gms1p in compartments that are sensitive to Brefeldin A. Btn1p function might be linked to that of Vps34p, a phosphatidylinositol 3-kinase, because Btn1p acts as a multicopy suppressor of the severe Cpy1p vacuole protein-sorting defect of *vps34*Δ cells. Together, these results indicate an important role for Btn1p in the Golgi complex, which affects Golgi homeostasis and vacuole protein sorting. We propose a similar role for CLN3 in mammalian cells.

Supplementary material available online at
http://jcs.biologists.org/cgi/content/full/122/8/1163/DC1

Key words: *CLN3*, *btn1*, Batten, Neuronal ceroid lipofuscinosis, *vps10*, Carboxypeptidase Y, Vacuole, Golgi, Neurodegeneration, *S. pombe*

Introduction

Juvenile-onset neuronal ceroid lipofuscinosis (JNCL), or Batten disease, is one of a group of severe neurodegenerative lysosomal storage disorders characterised by accumulation of ageing-associated lipofuscin-like material in the lysosomes of most cells. JNCL typically presents between the ages of 6 to 10 years with visual failure, followed by epilepsy and progressive cognitive and motor deterioration as a result of selective neuronal cell loss, and is caused by mutations in the *CLN3* gene (The International Batten Disease Consortium, 1995). CLN3 is a multi-pass transmembrane protein (Kyttälä et al., 2004; Nugent et al., 2008; Storch et al., 2007), which has proved difficult to detect at endogenous levels using currently available antibodies, perhaps because of low expression or inaccessibility of the epitopes. The use of protein overexpression systems has led to the assumption that CLN3 is a lysosomal membrane protein (Ezaki et al., 2003; Haskell et al., 2000; Järvelä et al., 1999; Järvelä et al., 1998; Kyttälä et al., 2004; Luiro et al., 2001; Persaud-Sawin et al., 2007). CLN3 has been functionally linked to diverse cellular processes, including lysosomal homeostasis (Holopainen et al., 2001; Pohl et al., 2007; Ramirez-Montealegre and Pearce, 2005), autophagy (Cao et al., 2006), lipid synthesis or modification (Hobert and Dawson, 2007; Narayan et al., 2006), cytoskeletal organisation (Luiro et al., 2004), apoptosis (Persaud-Sawin et al., 2002), trafficking (Fossale et al., 2004), and, most recently, HIV infection (Brass et al., 2008). Despite these endeavours, the function of CLN3 remains elusive.

The conservation of CLN3 in single-celled eukaryotes suggests that it has a fundamental role in eukaryotic cells. To help understand its function, we used a simple model system, the fission yeast *Schizosaccharomyces pombe*. We previously showed that deletion of *btn1*, the fission yeast orthologue of *CLN3*, affects vacuole homeostasis, causing an increase in the size of the vacuoles, which are equivalent to lysosomes (Kitzmüller et al., 2008), and a decrease in vacuole pH (Gachet et al., 2005), as occurs in cells from a JNCL patient (Holopainen et al., 2001). Importantly, and validating our approach, Btn1p and CLN3 have been shown to be functional orthologues, because expression of CLN3 is able to rescue multiple defects of *btn1*Δ cells (Codlin et al., 2008b; Gachet et al., 2005). Similarly, *BTN1*, the orthologous gene from *Saccharomyces cerevisiae*, has also been implicated in vacuole homeostasis (Chattopadhyay et al., 2000; Kim et al., 2003; Padilla-Lopez and Pearce, 2006; Pearce et al., 1999; Pearce and Sherman, 1998), as well as in the response to oxidative stress (Osorio et al., 2007).

In *S. pombe*, GFP-Btn1p traffics unusually slowly to the vacuole (Gachet et al., 2005), compared with other vacuole membrane proteins (Bellemare et al., 2002; Gaits and Russell, 1999; Iwaki et al., 2003). At steady state, Btn1p is not predominantly localised to the vacuole, but is mainly located in unidentified prevacuole compartments (Gachet et al., 2005). Trafficking studies in a *ypt7*-null strain, defective for fusion with the vacuole, showed that Btn1p has a functional role in these prevacuole compartments that affects vacuole homeostasis (Gachet et al., 2005). This was the first clear indication that Btn1p (and, therefore, possibly CLN3) has a function that is not at the vacuole or lysosome. This might underlie the pleiotropic phenotypes previously recognised in cells deleted for *btn1* (Codlin et al., 2008a; Codlin et al., 2008b; Gachet et al., 2005).

Since Btn1p is involved in vacuole homeostasis in both *S. pombe* (Gachet et al., 2005) and *S. cerevisiae* (Kim et al., 2003; Pearce et al., 1999; Pearce and Sherman, 1998), and all NCL genes affect lysosomal function, with some encoding lysosomal hydrolases, we wondered whether Btn1p has a role in the trafficking of vacuole-bound hydrolases. The best-studied vacuole protein-sorting (*vps*) pathway in yeasts is that of the hydrolase carboxypeptidase Y (Cpy1). The major sorting receptor for this hydrolase is the type 1 receptor Vps10p (official symbol Pep1p) (Iwaki et al., 2006), which binds Cpy1p in the *trans*-Golgi network (TGN) and releases it in late endosomes for onward trafficking to the vacuole. Recycling of Vps10p back to the TGN for further rounds of Cpy1p sorting is dependent on the retromer complex (Iwaki et al., 2006), and expression of Vps10p in retromer deletion strains, e.g. *vps26*Δ, causes it to be mistargeted to the vacuole membrane, because it can no longer be recycled back to the TGN. Cpy1p trafficking is used as a marker phenotype of vacuole protein-sorting defects, and mis-sorting of Cpy1p at any stage of this pathway, for example by deletion of *vps10* or retromer components, leads to its secretion from the cell (Iwaki et al., 2006; Robinson et al., 1988; Rothman and Stevens, 1986).

In this study, we found that Btn1p in *S. pombe* is required for vacuole protein sorting of Cpy1p and for post-Golgi trafficking of its receptor, Vps10p. It is also implicated in other Cpy1p vacuole protein-sorting pathways. Furthermore, we show that this might occur through a direct effect on the Golgi compartment, because Btn1p is predominantly located in the Golgi complex at steady state, and changes in the level of expression of *btn1* affect the number, location and morphology of these compartments.

Results

*btn1*Δ cells are defective in vacuole protein-sorting of Cpy1p

We examined the effect of deletion of *btn1* on the trafficking of the vacuole hydrolase Cpy1p. A defect in its sorting results in secretion from the cell (Iwaki et al., 2006). To assess this, we used cells that were actively growing in log phase and performed colony blot assays using a *S. pombe*-specific anti-Cpy1p antibody (Tabuchi et al., 1997) to detect secreted Cpy1p. The *cpy1*Δ strain was included as a negative control for the antibody, and the *vps26*Δ or *vps10*Δ strains as positive controls, because both secrete easily detectable levels of Cpy1p (Iwaki et al., 2006). We found that the *btn1*Δ strain secreted Cpy1p protein, whereas wild-type cells secrete only a minimal amount of Cpy1p (Fig. 1A). The amount of Cpy1p secreted by *btn1*Δ cells was consistent over several experiments and, as determined by densitometry (Fig. 1B), was similar to the moderate amount secreted by the retromer mutant strain *vps26*Δ, in which Vps10p cannot be recycled back to the TGN, and was slightly less than that of *vps10*Δ cells, which lack its major sorting receptor. Thus, *btn1*Δ cells exhibit a moderate Cpy1p sorting defect.

Deletion of *btn1* affects Vps10p trafficking

We considered how Btn1p affects vacuole protein sorting of Cpy1p. First, we monitored the location of its sorting receptor, Vps10p, in the *btn1*Δ strain. In wild-type cells, Vps10p predominantly localises to multiple cytoplasmic punctae (Fig. 2A), typical of the Golgi or TGN (Iwaki et al., 2006). By contrast, in *btn1*Δ cells, we observed a reduced number of punctae and the appearance of structures that were perinuclear and cortical, with ribbon-like connective tubules (Fig. 2B), typical of the *S. pombe* endoplasmic reticulum (ER) (Gachet et al., 2005; Pidoux and Armstrong, 1993; Vjestica et al., 2008) (supplementary material Fig. S1A). An ER-like pattern was observed in 47% of cells expressing Vps10p, with the remainder displaying both ER and punctate staining. These data suggest that the steady state localisation of Vps10p is altered in the absence of *btn1*.

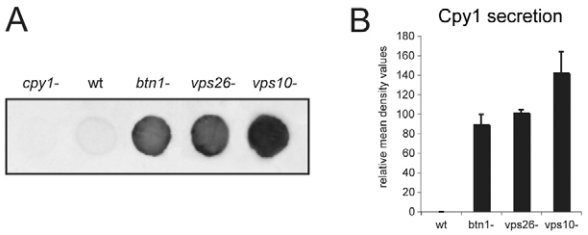

Fig. 1. *btn1* is required for vacuole protein sorting of the vacuole peptidase Cpy1p. Colony blot assay of indicated cells grown for 6 hours on YES agar using *S. pombe* specific anti-Cpy1p antibody. *btn1*Δ cells abnormally secrete Cpy1p. (A) Colony blot of indicated cells showing minimal Cpy1 secretion from wild-type (wt) cells but secretion from *btn1*Δ, *vps26*Δ and *vps10*Δ cells. (B) Bar chart depicting mean (± s.d.) density values relative to wild-type levels of Cpy1p secretion in colony blot assays (mean of three experiments).

We explored this location defect further. We compared the trafficking and final location of Vps10p after its expression was repressed by the incorporation of thiamine into the medium (which inhibits the *nmt* promoter system of the pREP expression plasmids). In wild-type cells, most ectopically expressed Vps10p was re-routed to the vacuole within 3 hours of promoter repression (Fig. 2C), although some punctate stained compartments remained. This is probably due to protein turnover or saturation of the retromer system, such that excess Vps10p is degraded at the vacuole, as previously demonstrated (Cereghino et al., 1995; Iwaki et al., 2006). By contrast, gene repression studies in *btn1*Δ cells did not have the same effect. In these cells, Vps10p was not evident at the vacuole after 3 hours (Fig. 2D), nor was it retained in the ER. Instead, Vps10p was held within a few distinct cytoplasmic compartments. These compartments did not resemble endocytic compartments, because of their low number and dispersed location, but did resemble those of the *S. pombe* Golgi complex (Vjestica et al., 2008). To confirm the identity of these compartments, we treated these *btn1*Δ cells with brefeldin A (BFA). BFA causes the Golgi complex (*cis*-, medial- and *trans*-Golgi), but not the *trans*-Golgi network (TGN) or later compartments, to be redistributed back to the ER (Brazer et al., 2000), as in mammalian cells (Lippincott-Schwartz et al., 1989). This effect is due to inhibition of Arf1p-dependent vesicle formation. The TGN remains unaffected. We found that, upon BFA treatment, the bright Vps10p-containing punctae of *btn1*Δ cells (Fig. 2E) were replaced by the classic perinuclear and cortical ER pattern (Fig. 2F), as observed with BFA treatment of Golgi markers Gms1p and Anp1p (supplementary material Fig. S2A; Fig. 2B). This indicates that the observed punctae, before BFA treatment, are Golgi compartments. The same treatment in wild-type cells, in which Vps10p had trafficked for 3 hours following gene repression, had no effect on the location of Vps10p (Fig. 2G), which by this time had exited the Golgi and TGN and was predominantly at the vacuole (Fig. 2C). Together, these data show that, in the absence of *btn1*, Vps10p is delayed in its trafficking through the ER and Golgi, and that its exit from the Golgi, and progression to the TGN and into the *vps* pathway, is severely impeded.

Btn1p localises to the Golgi complex

Btn1p has a functional role in previously unidentified prevacuole compartments that affects vacuole function (Gachet et al., 2005), and here we have shown that Btn1p is required for Cpy1 sorting and exit of Vps10p from the Golgi. We therefore explored whether the prevacuole location of Btn1p was at the Golgi complex. We found extensive colocalisation of GFP-Btn1p with the Golgi marker Gms1p-CFP at steady state in wild-type cells (Fig. 3A), with few compartments exclusive for Gms1p or Btn1p (Fig. 3B). This colocalisation was observed at low levels of expression of GFP-Btn1p (Fig. 3A, asterisk) as well as at higher levels (remaining cells), making it unlikely to be due to protein overexpression. This Golgi localisation was found to be specific to the native protein, because Btn1p containing the equivalent of a JNCL disease mis-sense mutation, Gly187Ala (Btn1p^{G136A}) (www.ucl.ac.uk/ncl/cln3.shtml), which affects trafficking (Gachet et al., 2005), did not colocalise with Gms1p (Fig. 3C). Rather, this mutant protein was retained within structures typical of the *S. pombe* ER. Hence, ectopically expressed GFP-Btn1p resides predominantly at the Golgi compartment.

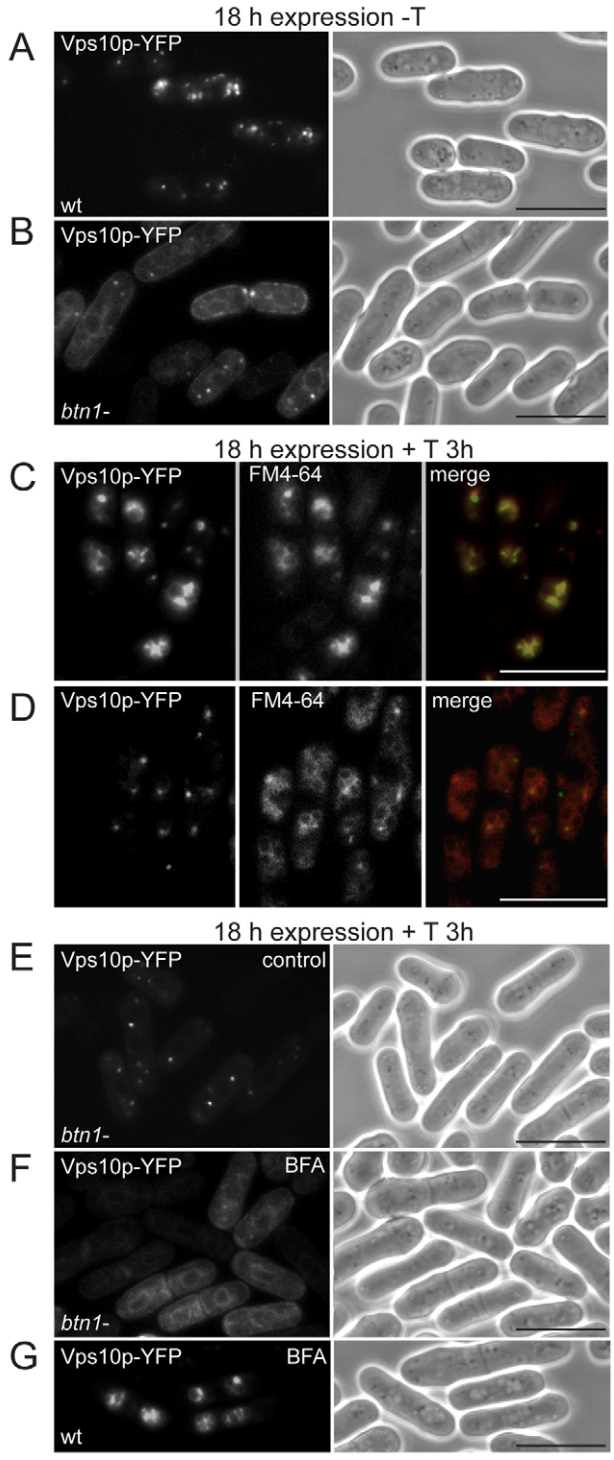

Btn1p is located in an earlier Golgi compartment than Vps10p

To confirm that the compartments in which Btn1p colocalised with Gms1p were indeed the Golgi, we treated these cells with BFA. Exposure to BFA caused GFP-Btn1p (Fig. 4A) to redistribute back to the ER within 1 hour, as previously shown for the Golgi markers Gms1p (supplementary material Fig. S2A) or Anp1p (supplementary material Fig. S2B). By contrast, Vps10p-YFP remained in punctate cytoplasmic compartments, with minimal ER localisation (Fig. 4B), even after 2 hours of BFA treatment (data not shown). Btn1p, therefore, is predominantly located within the Golgi complex, whereas Vps10p is predominantly located in later compartments, probably TGN, but possibly endosomal compartments, between which it cycles. These data are consistent with the Gms1p colocalisation (Fig. 3A; Fig. 4C,D), since Vps10p was more often found in punctate structures adjacent to Gms1p-positive Golgi compartments, rather than in these compartments. In addition, unlike Vps10p (supplementary material Fig. S3A; Fig. 4F), Btn1p was not misrouted to the vacuole in the absence of functional retromer: as in *vps26*Δ cells, it remained in pre-vacuolar Golgi compartments (supplementary material Fig. S3B) that were sensitive to BFA treatment (Fig. 4E).

Excess Btn1p, similarly to excess Vps10p (Cereghino et al., 1995; Iwaki et al., 2006), is eventually targeted to the vacuole, possibly for degradation, because, after prolonged gene repression of GFP-Btn1p in wild-type cells, GFP-Btn1p was detected only at the vacuole (supplementary material Fig. S3C). Exposure to BFA did not affect the localisation of either Btn1p or Vps10p that had already reached the vacuole (after trafficking) following gene repression (supplementary material Fig. S3D; Fig. 2G).

Fig. 2. *btn1* mediates exit of Vps10p from the Golgi. (A,B) Delayed trafficking of Vps10p in *btn1*Δ cells: fluorescence images of wild-type (wt, A) or *btn1*Δ cells (B) expressing Vps10p-YFP showing defective trafficking in *btn1*Δ cells (mainly ER or Golgi rather than the TGN distribution typical of wild-type cells). (C,D) Vps10p is prevented from entering the TGN-to-vacuole pathway in the absence of *btn1*: fluorescence images of wild-type (wt, C) or *btn1*Δ cells (D) overexpressing Vps10p-YFP after 3 hours of thiamine-induced promoter repression and FM4-64 vacuole labelling showing Vps10p is retained within cytoplasmic Golgi-like compartments in *btn1*Δ cells. (E,F,G) Vps10p is delayed within the Golgi in the absence of *btn1*. Fluorescence images of *btn1*Δ cells expressing Vps10p-YFP after 3 hours of thiamine-induced promoter repression (E) and after 1 hour of Brefeldin A (BFA) treatment (F) showing that these Vps10p-containing compartments are not post-Golgi because they collapse back to the ER. Vps10p can exit the Golgi in wild-type cells. (G) Fluorescence images of wild-type (wt) cells expressing Vps10p-YFP after 3 hours of thiamine-induced promoter repression and 1 hour of Brefeldin A (BFA) treatment, showing that these Vps10p-containing compartments are not Golgi because they are unaffected by BFA treatment. Scale bars: 10 μm.

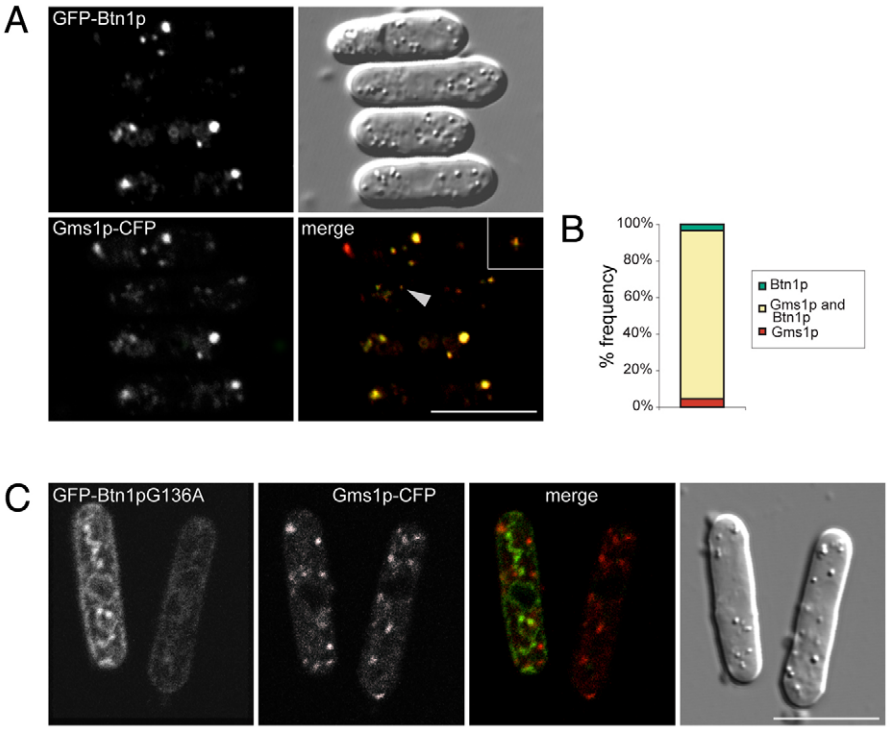

Fig. 3. Btn1 localises to the Golgi compartment. (A) GFP-Btn1p colocalises extensively with Gms1p-CFP. Confocal images showing wild-type cells expressing Gms1p-CFP and GFP-Btn1p (asterisk indicates a cell expressing GFP-Btn1p at low levels, and the arrowhead a puncta magnified three times in the inset). (B) Bar chart depicting percentage of compartments (n>200) containing indicated proteins. (C) GFP-Btn1p^{G136A} mutant protein does not colocalise with Gms1p. Confocal images of wild-type cells expressing Gms1p-CFP and GFP-Btn1p^{G136A}. Scale bars: 10 μm.

Golgi number and positioning defects in *btn1*Δ cells

Given the predominant location of expressed Btn1p in the Golgi compartment, and since Golgi exit of Vps10p appears to be the most upstream defect so far described in *btn1*Δ cells, we tested whether absence or overexpression of Btn1p affected the Golgi compartments in any way. For this, we monitored the location and number of Gms1p-positive Golgi structures by fluorescence microscopy. Since these compartments can vary in size, location and number according to the stage of the cell cycle (Ayscough et al., 1993; Vjestica et al., 2008), we monitored those compartments only in similarly sized interphase cells, in one focal plane that bisected the nucleus. Despite the slightly diffuse background associated with this CFP marker, we observed highly significant differences in the number and positioning of the visible punctate Gms1p-positive Golgi compartments between wild-type and *btn1*Δ cells. First, there were fewer Gms1p-punctae in *btn1*Δ cells, with an average of four per field of view, compared with seven in wild-type cells (Fig. 5A,B). We also noted that one or two of these punctae were particularly prominent in *btn1*Δ cells. Maximum projection images of 0.3 μm z-sections through *btn1*Δ and wild-type cells expressing Gms1p-CFP were used to display all Golgi compartments (supplementary material Fig. S4), and these and the corresponding movies (supplementary material Movies 1 and 2) confirmed a reduction in the total number of Golgi compartments in *btn1*Δ cells compared with wild-type cells (Vjestica et al., 2008). Thus, loss of *btn1* had an impact on the number of Golgi compartments.

We also determined and compared the intracellular positioning of Golgi compartments in these cells by counting the numbers of Gms1p-positive punctae present with respect to their distance from the nucleus, and allocating these into one of five regions (with ‘a’ being furthest away, at the tip, and ‘e’ being closest to the nucleus). Wild-type cells had most Golgi in the cell body (regions b-d). By contrast, *btn1*Δ cells displayed more Golgi at the cell tip region (region a) (33% compared with 10% in wild-type cells), and less in a perinuclear location (region e) (4% compared with 10% in wild-type cells) (Fig. 5C). This was also confirmed by maximal projection images (supplementary material Fig. S4). Thus, loss of *btn1* has an impact on Golgi positioning within the cell.

Interestingly, cells overexpressing Btn1p also exhibited some defects in Golgi compartment distribution (Fig. 3A; Fig. 5C), similarly to that of the *btn1*Δ strain (Fig. 5C), with more Gms1p-positive Golgi compartments at the cell tip region and less at the perinuclear region, when compared with wild-type cells. Also, although the number of Golgi compartments was not significantly different from that of wild-type cells, we again noted that one or two compartments per cell were visibly brighter and possibly larger (Fig. 3A). This could be due to a change in size or morphology of these compartments. Overall, therefore, our data suggest that the level of expression of Btn1 protein affects Golgi homeostasis.

btn1 affects Golgi morphology

To define the effects of *btn1*, we used electron microscopy to compare the morphology of the Golgi complex between wild-type and *btn1*Δ cells. The morphology of *S. pombe* Golgi resemble those of mammalian cells (Chappell and Warren, 1989). In wild-type cells, the multiple Golgi were easily recognisable as electron-dense ribbons or flattened cisternae of length ~0.5-0.8 μm, often with a globular (or beaded) appearance (Fig. 6A,B). Most had one, two or three adjacent ribbons, and occasionally more (Fig. 6E), and were distributed throughout the cytoplasm, often near the nucleus (Fig. 6A,B). There were few Golgi that did not have this typical ultrastructure. By contrast, in *btn1*Δ cells, there were less recognisable Golgi per cell, the ribbons of these were slightly longer (>1 μm) (Fig. 6C,D), and there were fewer with three or more adjacent cisternae (Fig. 6E). There was, however, an increase in the number of structures that appeared to be misshapen Golgi (34%

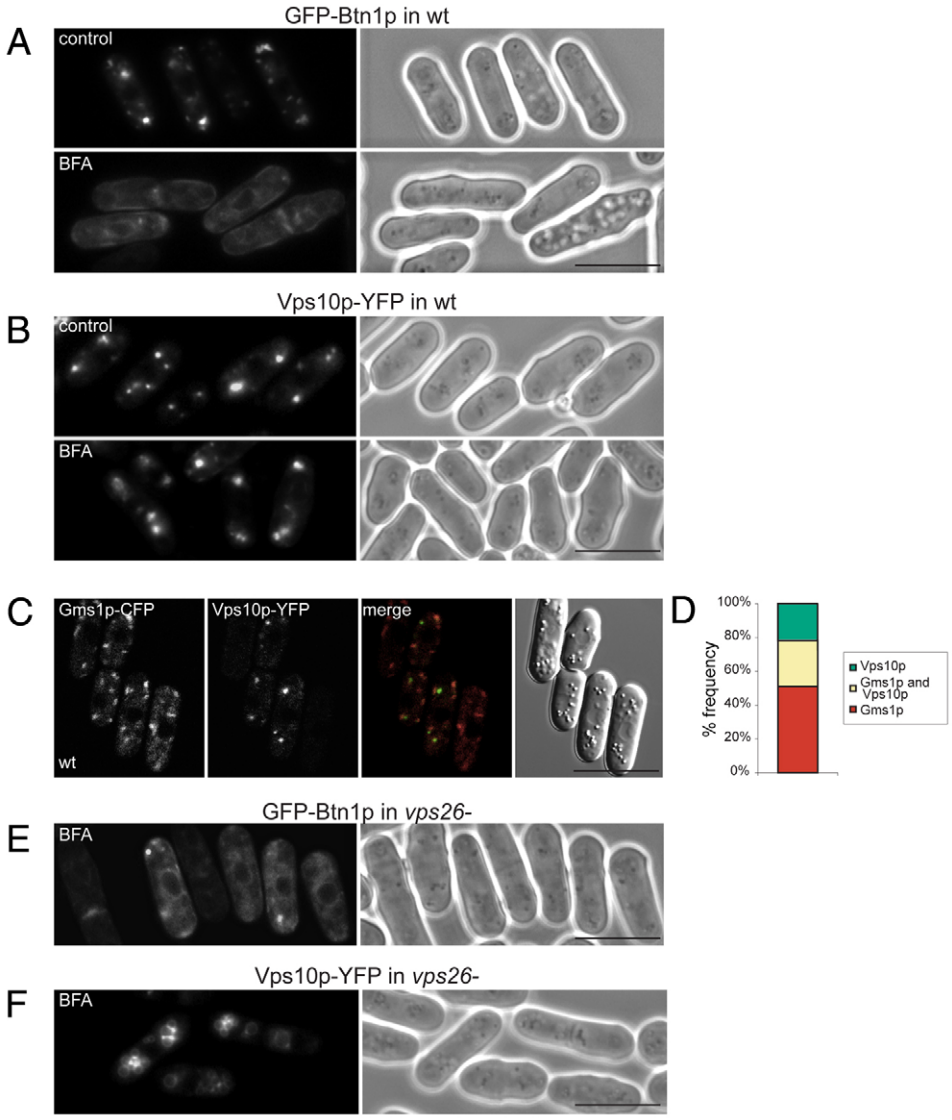

Fig. 4. Btn1p localises upstream of Vps10p. (A,B) Btn1p localises to the Golgi compartment in wild-type cells, which is upstream of Vps10p. Fluorescence images of wild-type cells expressing GFP-Btn1p (A) or Vps10p-YFP (B) treated with Brefeldin A (BFA) or without (DMSO control) showing that Btn1p-containing Golgi compartments collapse back to the ER whereas Vps10p-containing compartments do not. (C) Most Vps10p is not located at the Golgi. Confocal images showing wild-type cells expressing Gms1p-CFP and Vps10p-YFP that do not colocalise. (D) Bar chart depicting percentage of compartments (n>200) containing indicated proteins. (E,F) Unlike Vps10p, Btn1p remains Golgi localised in the absence of a functional retromer complex, and is not misrouted to the vacuole. GFP-Btn1p (E) or Vps10p-YFP (F) expressed in *vps26*Δ cells and treated with BFA or without (DMSO control). All Btn1p-containing Golgi compartments collapse back to the ER whereas Vps10p-containing vacuole compartments do not. Scale bars: 10 µm.

compared with 5% in wild-type cells), some with extremely contorted and swollen compartments, often more than 1.3 µm in diameter across the whole structure. These Golgi were usually not located near the nucleus (Fig. 6C,D). Thus, deletion of *btn1* has a striking effect on Golgi morphology.

Btn1p may be required for more than one Cpy1 vacuole protein sorting pathway

To provide insight into the role and possible mechanism of action of *btn1,* we explored whether loss or increased expression of Btn1p affected the Cpy1p vacuole protein-sorting defect of *vps* strains deleted for *vps10*, *vps26* and *vps34*. First, we investigated the effect of loss of *btn1* on Cpy1p sorting in *vps* strains. We derived the double mutant strain, *vps10*Δ*btn1*Δ, and assayed for altered Cpy1p secretion compared with that in parental strains. Interestingly, significantly more Cpy1p was secreted when both *vps10* and *btn1* genes were deleted, in comparison to the parental strains (Fig. 7A,D). This suggests that Btn1p might act in more than one Cpy1p *vps* pathway. The amount of Cpy1p secreted was similar to that of the *vps34*Δ strain (Fig. 7B,D), which has the most severe Cpy1p sorting defect associated with deletion of a single gene (Iwaki et al., 2004; Tabuchi et al., 1997; Takegawa et al., 1995), presumably because, in addition to a direct effect on the *vps* pathway, Vps34p also acts at several other steps in the cell (Burda et al., 2002; Futter et al., 2001; Lawe et al., 2000; Wurmser and Emr, 2002; Yan and Backer, 2007; Zeng et al., 2006), including the Golgi (Deloche et al., 2001; Hall et al., 2006). These high levels of Cpy1p secretion from *vps10*Δ*btn1*Δ cells (Fig. 7D) suggest that loss of both *vps10* and *btn1* severely impacts the correct trafficking Cpy1p. We then derived the double deletion strain *vps34*Δ*btn1*Δ and, surprisingly, found that even more Cpy1p was secreted by cells deleted for both *vps34* and *btn1* than the parental strains (Fig. 7B and shorter exposure Fig. 7C,D). This supports the importance of *btn1* in more than one Cpy1p vacuole protein-sorting pathway. We also derived the double mutant strain *vps26*Δ*btn1*Δ, and found that the level of Cpy1p secreted from this strain was similar to that of both parental strains (Fig. 7B, Fig. 1C). This suggests that the Cpy1 secretion defect associated with loss of *btn1* affects the same pathway as the defect arising from that of a loss of retromer function. Considering the respective locations of Btn1p and retromer, Btn1p probably acts upstream of retromer.

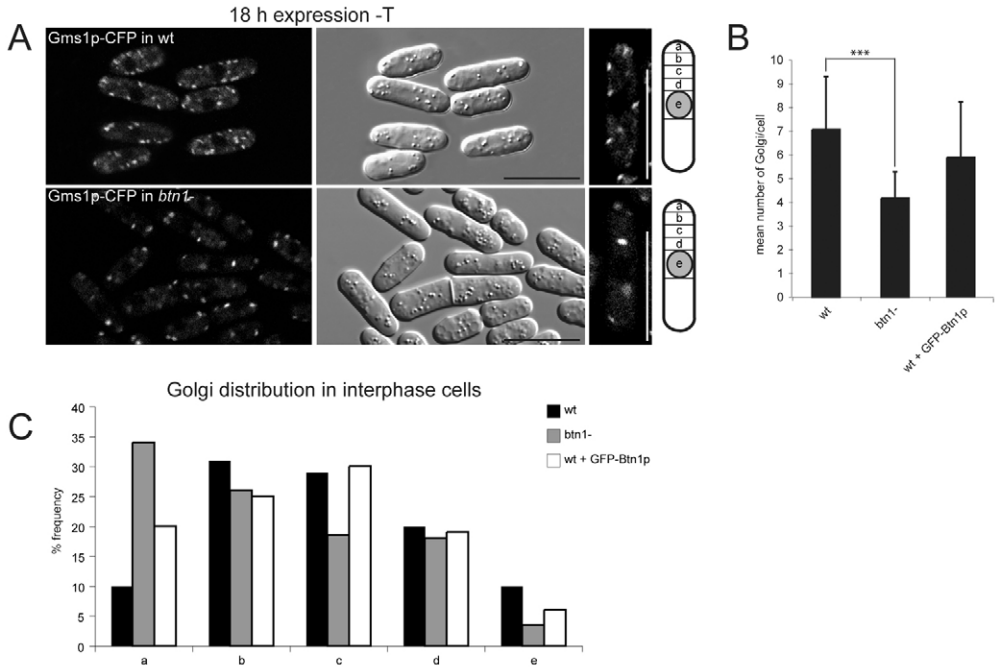

Fig. 5. Btn1p regulates Golgi number and positioning. Absence of *btn1* causes a reduction in the number of Gms1p-stained Golgi compartments. (A) Confocal images of wild-type (wt) *btn1*Δ cells expressing Gms1p-CFP showing reduced numbers of Golgi and positioning defects (end panel shows a single typical cell). (B) Bar chart of numbers of Golgi in wild-type (wt), *btn1*Δ cells and wild-type cells overexpressing Btn1p (n>200 Golgi across single cross-sections in three independent experiments); wild-type cells, 7.1±2.2; *btn1*Δ cells, 4.2±1.4; cells overexpressing Btn1p, 5.9±2.59; ***P<0.001. (C) Absence of *btn1* or ectopic expression of Btn1p alters the distribution of Golgi compartments. Bar chart of positions of Gms1p-stained Golgi compartments in wild-type (wt), *btn1*Δ cells and cells overexpressing Btn1p with respect to their distance from the nucleus. The cartoon in A illustrates the positions of regions counted (n>200 Golgi over three experiments). Scale bars: 10 μm.

Btn1p suppresses the Cpy1p secretion defect of *vps34*Δ cells

To investigate the effect of increased expression of Btn1p on Cpy1p sorting in *vps* strains, we first confirmed that the secretion defect of *btn1*Δ cells was rescued by ectopic expression of GFP-Btn1p (supplementary material Fig. S5Ai), which was predominantly localised to BFA-sensitive Golgi compartments in these cells, as in wild-type cells (supplementary material Fig. S5B), and which rescued other previously described pleiotropic phenotypes of *btn1*Δ cells (Codlin et al., 2008a; Codlin et al., 2008b; Gachet et al., 2005). This rescue was specific to native protein because there was no rescue by expression of GFP alone (empty vector), or GFP-Btn1p^{G136A} mutant protein, which was predominantly localised to the ER (Gachet et al., 2005). Importantly, the Cpy1p secretion defect of *btn1*Δ cells was also effectively rescued by expression of GFP-CLN3 (supplementary material Fig. S5Aii), further supporting the use of *S. pombe* as a model organism to understand CLN3 function.

The Cpy1 secretion defects of the *vps10*Δ cells and *vps26*Δ cells were not significantly altered by expression of Btn1p (Fig. 8A,B; supplementary material Fig. S6A), but did show a small increase in Cpy1p secretion. Interestingly, the Cpy1 secretion defect of the *vps34*Δ strain was significantly decreased by expression of Btn1p (Fig. 8A-C; supplementary material Fig. S6A,B), which was localised to BFA-sensitive Golgi complex in these cells, as in wild-type cells (supplementary material Fig. S5C). To confirm that this decrease in Cpy1p secretion by *vps34*Δ cells was a result of Btn1p activity, we expressed the mutant GFP-Btn1p^{G136A} protein in this strain. Expression of this mutant Btn1p protein in *vps34*Δ cells did not rescue the Cpy1p secretion defect of *vps34*Δ cells; rather, the level of Cpy1p secretion was significantly increased (Fig. 8C,D; supplementary material Fig. S6B), perhaps because of its location in the ER (supplementary material Fig. S5D). This suggests that excess mutant Btn1p protein further exacerbated the secretion defect of *vps34*Δ cells, consistent with the Cpy1 secretion data observed for the *vps34*Δ *btn1*Δ double mutant strain (Fig. 8C,D and Fig. 7D). To confirm that these effects were due to expression of these proteins, we inhibited their expression in *vps34*Δ cells using thiamine and performed colony blots of those cells, and found that there was now no difference in Cpy1p secretion (Fig. 8E,F; supplementary material Fig. S6B). Overall, these data suggest that the action of Btn1p can compensate for, or bypass, a lack of phosphatidylinositol 3-kinase activity in Cpy1p sorting.

Discussion

The function of the human disease gene *CLN3* remains elusive, more than a decade after it was first identified. Here, we provide evidence that *btn1*, the *S. pombe* orthologue of *CLN3*, is involved in mediating vacuole protein sorting of the hydrolase carboxypeptidase Y, and can therefore be considered a novel *vps* protein. Mis-sorting of Cpy1p in the absence of *btn1* appears to be due, at least in part, to a severe defect in trafficking of the Cpy1 sorting receptor Vps10p from the Golgi to the TGN, where sorting of Cpy1p normally occurs. This leads to Cpy1p secretion, as depicted in our model (Fig. 9), and is the most upstream defect yet described for Btn1p, and by extrapolation, CLN3.

Our data also implicate *btn1* in other, as yet unidentified, *vps10*-independent mechanisms of vacuole protein sorting, because loss of *btn1* in the *vps10* deletion strain exacerbated its Cpy1p secretion defect. This requires further study. Btn1p might be required for the

exit of other type 1 receptor proteins from the Golgi, in addition to Vps10p, and possibly other proteins. Although much is now known about transport within the Golgi compartment (Donaldson et al., 2005; Patterson et al., 2008), and out of the TGN (De Matteis and Luini, 2008; McNiven and Thompson, 2006), less is known about transport between the Golgi compartment and the TGN. It might involve vesicular transfer, fusion of *trans*-Golgi subdomains with the TGN, or maturation of *trans*-Golgi cisternae into the TGN. Additionally, recycling of some components from the TGN back to the Golgi has been proposed (Schaub et al., 2006). Deciphering the as yet unknown mechanism of action of Btn1p should facilitate further understanding of these pathways, and trafficking of Vps10p and other proteins.

We previously showed that Btn1p affects vacuole size and pH from prevacuole compartments (Gachet et al., 2005). We have now identified these as the Golgi complex, because they are sensitive to BFA, and because Btn1p extensively colocalises with the Golgi membrane-resident protein UDP-galactose transporter (Gms1p), part of the SLC35A family, which transport nucleotide sugars from the cytosol into the Golgi (Tanaka and Takegawa, 2001). We propose that Btn1p acts primarily at the Golgi compartment, where it is important for downstream *vps* pathways that consequently impact vacuole function. Data from the study supporting include: (1) the retardation of Vps10p in the Golgi when *btn1* is deleted; (2) the rescue of the Cpy1p sorting defect and vacuole defects by Btn1p located predominantly in a BFA-sensitive compartment; (3) the lack of rescue of these phenotypes upon expression of the Btn1p^{G136A} mutant protein; (4) the effect on the number and location of Golgi compartments when *btn1* is deleted; and (5) the aberrant Golgi structures visualised by EM in *btn1*Δ cells. We can also infer that the level of expression of Btn1p matters and is likely to be tightly regulated, because both its absence and overexpression affect the Golgi and vacuole compartments, and TGN-to-vacuole trafficking. Exactly how Btn1p affects Golgi size, positioning and structure remains to be determined. Btn1p may be more important for older or more active Golgi, because the number of stacks, as well as the total number of Golgi, is thought to increase during the cell cycle (Ayscough et al., 1993; Vjestica et al., 2008), and it is these structures that appear to be most affected in *btn1*Δ cells.

Some clues to Btn1p action might be provided by the discovery that it acts as a multicopy suppressor of *vps34*, because overexpression of Btn1p in *vps34*Δ cells specifically overcomes the severe mis-sorting of Cpy1p (Tabuchi et al., 1997). Vps34p, a phosphatidylinositol 3-kinase that makes phosphatidylinositol 3-phosphate, or some of its recruited downstream effectors, are known to affect many cellular processes, including events at the Golgi (Deloche et al., 2001; Hall et al., 2006; Ridley et al., 2001) and trafficking to the vacuole (Kihara et al., 2001; Stack et al., 1995; Takegawa et al., 1995). Expression of Btn1p might facilitate the

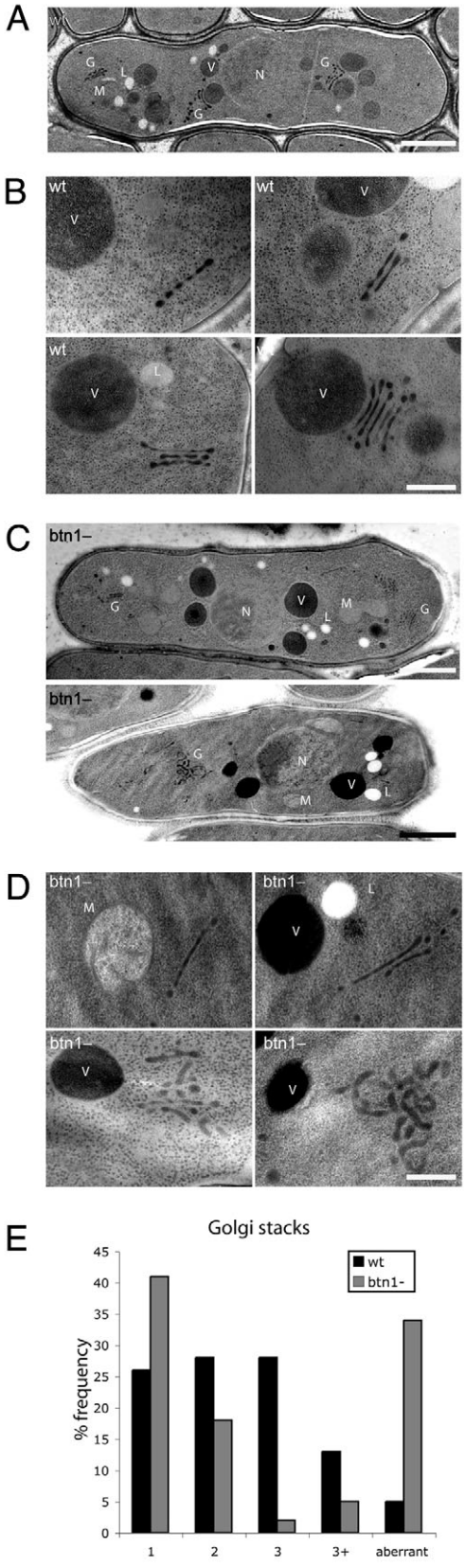

Fig. 6. *btn1* affects Golgi morphology. (A,B) Typical Golgi in wild-type (wt) cells have electron-dense ribbon-like flattened cisternae, often arranged in stacks. (A) Electron micrograph of a single cell at log phase, showing distribution of multiple Golgi (G, Golgi; L, lipid droplet; M, mitochondrion; N, nucleus; V, vacuole). Scale bar: 2 µm. (B) Electron micrographs of Golgi with single or multiple adjacent cisternae. Scale bar: 0.5 µm. (C,D) Typical Golgi in *btn1*Δ cells are longer and have fewer stacks, or have swollen and mis-shapen cisternae. (C) Electron micrographs of single cells at log phase showing fewer and less-prominent Golgi. Scale bars: 2 µm. (D) Electron micrographs of recognisable Golgi with stacked cisternae, and examples of larger aberrant Golgi structures. Scale bar: 0.5 µm. (E) *btn1*Δ cells have many atypical Golgi and fewer Golgi with multiple stacked cisternae. Bar chart of % frequency of Golgi complexes with defined numbers of stacks (1, 2, 3 or more), or those with aberrant morphology, in log-phase wild-type and *btn1*Δ cells [wt, *n*=43 Golgi (21 cells); *btn1*Δ, *n*=48 Golgi (28 cells)].

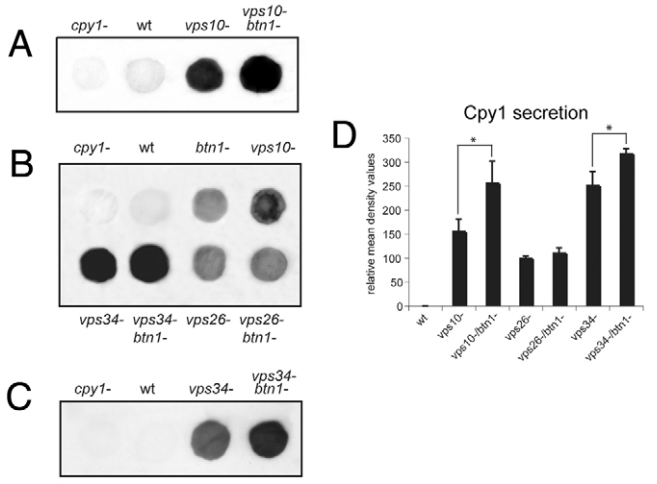

Fig. 7. *btn1* might be required for other *vps* pathways. (A) Btn1 might also be involved in a second vacuole protein-sorting pathway for Cpy1p. Colony blot assay of indicated cells grown on YES agar plates showing increased Cpy1p secretion from a *vps10*Δ*btn1*Δ double deletion strain compared to *vps10*Δ. (B) Colony blot assay of indicated double deletion strains showing that *vps26*Δ and *vps26*Δ*btn1*Δ cells secrete similar amounts to parental strains, but that *vps34*Δ*btn1*Δ cells secrete more than parental strains as observed in C at a lower exposure. (D) Bar chart depicting mean density values relative to wild-type levels of Cpy1p secretion in colony blot assays (mean ± s.d. of three experiments). **P*<0.05.

action of one or more of these effectors, permit bypass of a particular *vps34*-dependent pathway, or relieve a Golgi defect.

Interestingly, because vacuole defects associated with loss of *btn1* can be rescued by growth in acidic media (pH 4) (Gachet et al., 2005), as can the Cpy1p mis-sorting defect (our unpublished data), we cannot rule out a role for Btn1p in pH homeostasis, with alteration of Btn1p levels perhaps affecting the ionic environment within the lumen of the Golgi complex. This might, in turn, affect protein and lipid modification of receptors or cargo, or membrane remodelling and budding, causing the observed defect in Golgi structure, and leading to the retention of proteins such as Vps10p within the Golgi, and downstream sorting defects. This could be via a direct affect, because Btn1p shares distant sequence homology with transporters (Baldwin et al., 2004; Finn et al., 2006; Lobley et al., 2007), or, more likely, by affecting the activity or trafficking of transporters or channels, including those known to cause NCL (Cooper et al., 2006; Siintola et al., 2006; Siintola et al., 2007). Consistent with this, Btn1p is a multicopy suppressor of the vacuole defects of V-type H^+ ATPase (v-ATPase)-null cells (Codlin et al., 2008a), as well as their Cpy1p missorting defect (our unpublished data). We recently reported that Btn1p is essential for growth of *S. pombe* at high temperatures, with failure to correctly polarise sterol-rich domains at the plasma membrane, because of defective formation and polarisation of F-actin patches, disruption of endocytosis, and loss of Myo1p localisation (Codlin et al., 2008b). It is plausible that, in addition to *vps* pathways, Btn1p is required for other post-Golgi trafficking pathways that are required to deliver key proteins, particularly at high temperatures. This remains to be investigated.

It also remains to be determined whether the effect of loss of *btn1* on Vps10p and Vps10p-independent trafficking affects the targeting and activity of other vacuole hydrolases, in addition to Cpy1p. This is likely, because Vps10p, a type 1 sorting receptor, is known to facilitate the trafficking of several vacuole hydrolases in yeasts (Cooper and Stevens, 1996). Vps10p has long been considered the functional equivalent of the mammalian mannose-6-phosphate receptor (M6PR), despite fundamental differences in cargo recognition (Dahms et al., 1989; Valls et al., 1990). However, the M6PR yeast homologue is more likely to be the product of the less-studied *mrl1* gene (Whyte and Munro, 2001). Our data suggests that loss of *btn1* will also affect the trafficking of Mrl1p, and the localisation of other vacuole hydrolases such as Isp6p and Psp3p (Iwaki et al., 2006), that might use this pathway.

Vps10p is now recognised as structurally and functionally similar to mammalian sortilins, a family of type 1 sorting receptors that act in transport pathways from the TGN, some of which have specialised functions in neurons. Since the TGN is the major protein-sorting compartment of the cell, the determination of the effect of mutations in *CLN3* on the localisation and trafficking of the sortilins and M6PRs and their cargoes, as well as on other

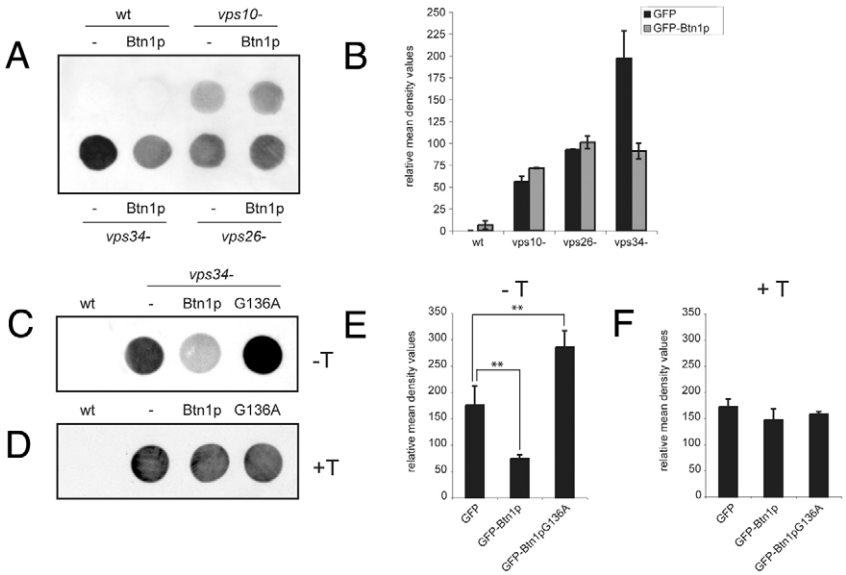

Fig. 8. Btn1p suppresses the Cpy1p secretion defect of *vps34*Δ cells. Ectopic expression of Btn1p rescues the Cpy1p secretion defect of *vps34*Δ cells but not that of *vps26*Δ or *vps10*Δ cells. (A) Colony blot assay of indicated cells grown on MM agar plates plus supplements for 6 hours. (B) Bar chart depicting mean density values relative to wild-type level of Cpy1p secretion of colony blot assays from indicated cells (mean of two experiments). (C-F) The rescue of the Cpy1p secretion defect of *vps34*Δ cells is specific to native Btn1p protein and to levels of protein expression: colony blot assay of indicated cells grown on MM agar plates plus supplements for 6 hours with native (Btn1p) or mutant $Btn1p^{G136A}$ protein in the absence (C) or presence (D) of thiamine (to repress expression). Bar charts depicting mean density values relative to wild-type level of Cpy1p secretion of colony blot assays from indicated cells without (E) and with (F) thiamine-induced promoter repression (mean ± s.d. of four and two experiments, respectively). ***P*<0.01.

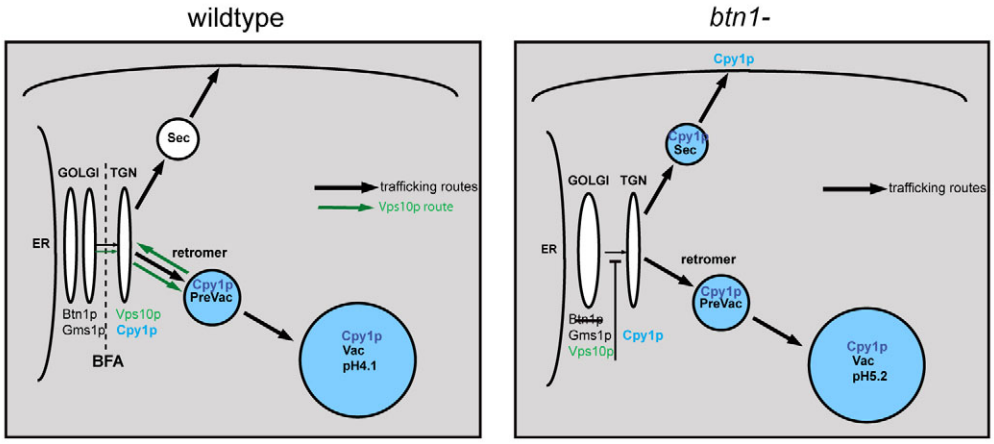

Fig. 9. Diagrammatic summary of the effect of loss of *btn1* on Vps10p trafficking and Cpy1p sorting. When *btn1* is deleted (right panel), Vps10p trafficking beyond the Golgi compartment to the TGN is impeded. Consequently, a proportion of Cpy1p is mis-sorted at the TGN and secreted. Black arrows represent established trafficking pathways. Green arrows in left panel represent the Vps10p trafficking or recycling pathway. BFA treatment causes compartments to the left of the dotted line to collapse back to the ER. Sec, secretory vesicles; Prevac, prevacuole compartment that is most likely a late endosome or multivesicular body; Vac, vacuole.

post-TGN carriers or routes, will be pertinent to the NCLs. By affecting some or all of these transport routes, mutations in *CLN3* or *btn1* might cause reduced levels of many enzymes in the lysosome or vacuole, affecting processing and maturation of important molecules and the degradative capacity of these organelles. These might include lysosomal hydrolases implicated in other types of NCL (Cooper et al., 2006; Siintola et al., 2006; Siintola et al., 2007). A thorough study of the lysosome proteome has not been performed in cells completely lacking CLN3 function. However, in JNCL cells, or in cells in which CLN3 function is substantially or partially reduced, alterations in trafficking or processing of specific lysosomal enzymes have been reported (Fossale et al., 2004; Junaid and Pullarkat, 1999; Metcalfe et al., 2008; Pohl et al., 2007; Sleat et al., 1998), and lysosomal homeostasis is affected (Holopainen et al., 2001; Kitzmüller et al., 2008; Ramirez-Montealegre and Pearce, 2005). In one instance, exit of a reporter version of the cation-independent M6PR from the TGN was significantly reduced when CLN3 was depleted (Metcalfe et al., 2008). Trafficking defects arising from CLN3 dysfunction might underlie other clinically significant phenotypic effects. For example, aberrant processing of amyloid precursor protein (APP) in neurons, a hallmark for Alzheimer's disease, also reported in JNCL (Golabek et al., 2000; Kitaguchi et al., 1990; Villanova et al., 1999; Wisniewski et al., 1992; Wisniewski et al., 1990), could be explained by defective trafficking of the sortilin SORL1 (Andersen et al., 2005).

Our findings do not necessarily contradict previous work in mammalian systems that concluded that the functional location for CLN3 was the lysosome. Endogenous levels of CLN3, like Btn1p, are low; hence the need for overexpression of CLN3, which might have distorted its subcellular distribution. Nevertheless, a recent study (Storch et al., 2007) concluded that, like Btn1p in *S. pombe*, trafficking of wild-type CLN3 to lysosomes was considerably slower than lysosome membrane-resident proteins, and that CLN3 remains in the Golgi compartment for a significant time. Indeed, a location of CLN3 in the Golgi has been noted previously (Haskell et al., 1999; Kremmidiotis et al., 1999). Importantly, yeast genetics have allowed us to study the effects of complete absence of *btn1*, which is particularly important in the light of our recent finding that cells from JNCL patients retain partial CLN3 function (Kitzmüller et al., 2008).

In conclusion, our data show that Btn1p, and by inference, CLN3, act in the Golgi compartment to affect the exit of at least one sorting receptor, thereby causing defective TGN-to-vacuole (lysosome) protein sorting. This important finding should help to uncover the mechanism of action of these proteins, and the precise consequences when such proteins are mutated.

Materials and Methods

Yeast strains and general techniques

Strains used in this study are listed in supplementary material Table S1. Media, growth, maintenance of strains and genetic methods were as described (Moreno et al., 1991). Cells were grown in rich medium (YES), or, for expression studies, in synthetic 'minimal' medium (MM) containing appropriate supplements. For protein expression experiments, cells were grown overnight in MM plus thiamine (4 μM), which inhibits expression from the *nmt* promoter. Cells were then washed three times in MM lacking thiamine, and grown in the same medium without thiamine, to allow expression and visualised at 18 hours. For gene repression studies, following overnight expression, plasmids were repressed by the addition of thiamine (4 μm final concentration), and cells grown for a further 3 hours or 6 hours, as indicated, before visualisation.

Fluorescence staining and microscopy

FM4-64 dye (Molecular Probes) was dissolved in DMSO at a concentration of 0.82 mM. 2 μl FM4-64 stock was added to 1 ml log phase cells grown as indicated (typically 2.5×10^6 cells/ml). For vacuole labelling, cells were exposed to FM4-64 for 30 minutes, washed, and chased for 40 minutes to allow all dye to reach the vacuole. For assessment of Golgi position and number, in three independent experiments, similarly sized interphase cells were monitored by confocal microscopy for the number and distribution of Gms1p-CFP-positive compartments in the focal plane that bisected the nucleus (n>200 Golgi for each independent experiment). Since this marker gave a diffuse background, only distinct punctae in that plane were counted, and the mean ± s.d. calculated [numbers were comparable to those in Vjestica et al. (Vjestica et al., 2008)]. Distribution was recorded by reference to distance from the centre of the nucleus. Maximum projection images of 0.3 μm z-sections through cells expressing Gms1p-CFP were used to display all Golgi compartments. The significance of changes in total Golgi number in one plane was assessed by performing unpaired Student's t-tests (95% confidence interval), using a critical P-value of 0.05. Images were visualised by either fluorescence or confocal microscopy, as indicated. Fluorescence microscopy was performed using a Hamamatsu digital camera C4742-95 fitted to a Zeiss Axioskop microscope with plan-Apochromat ×63 1.25 NA oil objective and images were recorded using OpenLab 3.4 software (Improvision). A FITC filter was used for GFP and YFP detection, and a Rhodamine filter for detection of FM4-64. Confocal images were acquired using a Leica TCS SPE confocal imaging system with plan-Apochromat ×63 1.25 NA oil objective and recorded using Leica LAS AF software. Images were opened and assembled in ImageJ. All images were downloaded to either Microsoft Excel for analysis, or to Adobe Photoshop 7 and Illustrator for assembly into montages. Z-stacks for movies (14 images acquired at 0.3 μm intervals) were captured by confocal microscopy and converted to avi images in ImageJ software for viewing in Quicktime. Maximum Z-projection images were obtained using ImageJ software.

Colony dot blots and western analysis

Immunoblot analysis to detect secreted Cpy1p was performed as described (Iwaki et al., 2006), with modifications. 1×10^7 cells were spotted onto nitrocellulose membrane laid on YES or MM agar plates and grown for indicated times, normally 6 hours at 25°C. After removing cells by washing, nitrocellulose membranes were subjected to immunodetection of Cpy1p using *S. pombe* specific anti-Cpy1p antibody (1:500), kindly provided by Dr Kaoru Takegawa, Kagawa University, Japan. Densitometry of colony blots was performed using a Bio-Rad GS-800 calibrated densitometer, and

measurements were acquired using QuantityOne software (Version 4.6). Typically, the density units over three independent experiments were recorded, the means calculated and plotted as relative mean density values ± s.d. (relative to wild-type levels), enabling comparison within and between experiments using the same experimental conditions (e.g. growth media). The significance of changes in Cpy1p secretion was assessed by performing unpaired Student's *t*-tests (95% confidence interval), using a critical *P*-value of 0.05. Protein expression was verified by fluorescence microscopy when the effect of this expression on Cpy1p secretion was under investigation.

Golgi inhibition

Brefeldin A (BFA, Sigma) (dissolved in DMSO at 10 mg/ml) was used to disrupt the Golgi complex. Briefly, BFA was added to equivalent numbers of log-phase cells in 1 ml at a final concentration of 100 μg/ml. Cells were rotated at 25°C and visualised at 1 hour or 2 hour intervals. Control experiments were performed using the equivalent concentration of DMSO.

High-pressure freezing EM using EMPACT system

Samples in log-phase growth were collected by filtration and immediately loaded into 1.5 mm hats and frozen under high pressure using the Leica EMPACT system (Leica, Vienna, Austria) according to the manufacturer's instructions. To visualise Golgi, freeze substitution was carried out using a Leica AFS freeze substitution unit with the following protocol: 2% osmium tetroxide in acetone at –90°C 6 hours, –60°C 6 hours, –30°C 6 hours, followed by an acetone wash –30°C to 20°C. Samples were embedded in epoxy resin (EPON; TAAB Laboratories). Sections were cut with a Leica Ultracut UCT microtome onto formvar-coated slot grids, stained with lead citrate, and viewed with a transmission electron microscope (TECNAI12: Philips, Eindhoven, The Netherlands). Images were acquired using a Morada digital camera (Olympus-SIS) and assembled in Adobe Photoshop. Golgi complexes were defined morphologically as electron-dense single or multiple adjacent ribbon-like tubules or cisternae.

We thank Kaoru Takegawa for supplying strains, plasmids and the anti-Cpy1p antibody; Snezhana Oliferenko for supplying strains; Lucy Collinson for assistance with EM; Rebecca Haines, Claudia Kitzmüller, Mark Marsh, Martin Raff and Katherine Bowers for helpful discussion. This work was supported by the Medical Research Council, UK (core support to the LMCB), the European Commission (503051), the Wellcome Trust, UK (067991, and Value in People Award with UCL) and UCL. We thank the Children's Brain Diseases Foundation, USA, for additional financial support. Deposited in PMC for release after 6 months.

References

Andersen, O. M., Reiche, J., Schmidt, V., Gotthardt, M., Spoelgen, R., Behlke, J., von Arnim, C. A., Breiderhoff, T., Jansen, P., Wu, X. et al. (2005). Neuronal sorting protein-related receptor sorLA/LR11 regulates processing of the amyloid precursor protein. *Proc. Natl. Acad. Sci. USA* **102**, 13461-13466.

Ayscough, K., Hajibagheri, N. M. A., Watson, R. and Warren, G. (1993). Stacking of Golgi cisternae in *Schizosaccharomyces pombe* requires intact microtubules. *J. Cell Sci.* **106**, 1227-1237.

Baldwin, S. A., Beal, P. R., Yao, S. Y., King, A. E., Cass, C. E. and Young, J. D. (2004). The equilibrative nucleoside transporter family, SLC29. *Pflugers Arch.* **447**, 735-743.

Bellemare, D. R., Shaner, L., Morano, K. A., Beaudoin, J., Langlois, R. and Labbe, S. (2002). Ctr6, a vacuolar membrane copper transporter in *Schizosaccharomyces pombe*. *J. Biol. Chem.* **277**, 46676-46686.

Brass, A. L., Dykxhoorn, D. M., Benita, Y., Yan, N., Engelman, A., Xavier, R. J., Lieberman, J. and Elledge, S. J. (2008). Identification of host proteins required for HIV infection through a functional genomic screen. *Science* **319**, 921-926.

Brazer, S. C., Williams, H. P., Chappell, T. G. and Cande, W. Z. (2000). A fission yeast kinesin affects Golgi membrane recycling. *Yeast* **16**, 149-166.

Burda, P., Padilla, S. M., Sarkar, S. and Emr, S. D. (2002). Retromer function in endosome-to-Golgi retrograde transport is regulated by the yeast Vps34 PtdIns 3-kinase. *J. Cell Sci.* **115**, 3889-3900.

Cao, Y., Espinola, J. A., Fossale, E., Massey, A. C., Cuervo, A. M., Macdonald, M. E. and Cotman, S. L. (2006). Autophagy is disrupted in a knock-in mouse model of juvenile neuronal ceroid lipofuscinosis. *J. Biol. Chem.* **281**, 20483-20493.

Cereghino, J. L., Marcusson, E. G. and Emr, S. D. (1995). The cytoplasmic tail domain of the vacuolar protein sorting receptor Vps10p and a subset of VPS gene products regulate receptor stability, function, and localization. *Mol. Biol. Cell* **6**, 1089-1102.

Chappell, T. G. and Warren, G. (1989). A galactosyltransferase from the fission yeast *Schizosaccharomyces pombe*. *J. Cell Biol.* **109**, 2693-2702.

Chattopadhyay, S., Muzaffar, N. E., Sherman, F. and Pearce, D. A. (2000). The yeast model for Batten disease: mutations in *BTN1*, *BTN2*, and *HSP30* alter pH homeostasis. *J. Bacteriol.* **182**, 6418-6423.

Codlin, S., Haines, R. L., Burden, J. J. E. and Mole, S. E. (2008a). *btn1* affects cytokinesis and cell wall deposition by independent mechanisms, one of which is linked to vacuole pH dysregulation. *J. Cell Sci.* **121**, 2860-2870.

Codlin, S., Haines, R. L. and Mole, S. E. (2008b). *btn1* affects endocytosis, polarisation of sterol-rich membrane domains and polarised growth in *Schizosaccharomyces pombe*. *Traffic* **9**, 936-950.

The International Batten Disease Consortium (1995). Isolation of a novel gene underlying Batten disease, *CLN3*. *Cell* **82**, 949-957.

Cooper, A. A. and Stevens, T. H. (1996). Vps10p cycles between the late-Golgi and prevacuolar compartments in its function as the sorting receptor for multiple yeast vacuolar hydrolases. *J. Cell Biol.* **133**, 529-541.

Cooper, J. D., Russell, C. and Mitchison, H. M. (2006). Progress towards understanding disease mechanisms in small vertebrate models of neuronal ceroid lipofuscinosis. *Biochim. Biophys. Acta* **1762**, 873-889.

Dahms, N. M., Lobel, P. and Kornfeld, S. (1989). Mannose 6-phosphate receptors and lysosomal enzyme targeting. *J. Biol. Chem.* **264**, 12115-12118.

De Matteis, M. A. and Luini, A. (2008). Exiting the Golgi complex. *Nat. Rev. Mol. Cell Biol.* **9**, 273-284.

Deloche, O., Yeung, B. G., Payne, G. S. and Schekman, R. (2001). Vps10p transport from the trans-Golgi network to the endosome is mediated by clathrin-coated vesicles. *Mol. Biol. Cell* **12**, 475-485.

Donaldson, J. G., Honda, A. and Weigert, R. (2005). Multiple activities for Arf1 at the Golgi complex. *Biochim. Biophys. Acta* **1744**, 364-373.

Ezaki, J., Takeda-Ezaki, M., Koike, M., Ohsawa, Y., Taka, H., Mineki, R., Murayama, K., Uchiyama, Y., Ueno, T. and Kominami, E. (2003). Characterization of Cln3p, the gene product responsible for juvenile neuronal ceroid lipofuscinosis, as a lysosomal integral membrane glycoprotein. *J. Neurochem.* **87**, 1296-1308.

Finn, R. D., Mistry, J., Schuster-Bockler, B., Griffiths-Jones, S., Hollich, V., Lassmann, T., Moxon, S., Marshall, M., Khanna, A., Durbin, R. et al. (2006). Pfam: clans, web tools and services. *Nucl. Acids Res.* **34**, D247-D251.

Fossale, E., Wolf, P., Espinola, J. A., Lubicz-Nawrocka, T., Teed, A. M., Gao, H., Rigamonti, D., Cattaneo, E., MacDonald, M. E. and Cotman, S. L. (2004). Membrane trafficking and mitochondrial abnormalities precede subunit c deposition in a cerebellar cell model of juvenile neuronal ceroid lipofuscinosis. *BMC Neurosci.* **5**, 57.

Futter, C. E., Collinson, L. M., Backer, J. M. and Hopkins, C. R. (2001). Human VPS34 is required for internal vesicle formation within multivesicular endosomes. *J. Cell Biol.* **155**, 1251-1264.

Gachet, Y., Codlin, S., Hyams, J. S. and Mole, S. E. (2005). *btn1*, the fission yeast homologue of the human Batten disease gene, *CLN3*, regulates vacuole homeostasis. *J. Cell Sci.* **118**, 5525-5536.

Gaits, F. and Russell, P. (1999). Vacuole fusion regulated by protein phosphatase 2C in fission yeast. *Mol. Biol. Cell* **10**, 2647-2654.

Golabek, A. A., Kida, E., Walus, M., Kaczmarski, W., Michalewski, M. and Wisniewski, K. E. (2000). CLN3 protein regulates lysosomal pH and alters intracellular processing of Alzheimer's amyloid-beta protein precursor and cathepsin D in human cells. *Mol. Genet. Metab.* **70**, 203-213.

Hall, B. S., Gabernet-Castello, C., Voak, A., Goulding, D., Natesan, S. K. and Field, M. C. (2006). TbVps34, the trypanosome orthologue of Vps34, is required for Golgi complex segregation. *J. Biol. Chem.* **281**, 27600-27612.

Haskell, R. E., Derksen, T. A. and Davidson, B. L. (1999). Intracellular trafficking of the JNCL protein CLN3. *Mol. Genet. Metab.* **66**, 253-260.

Haskell, R. E., Carr, C. J., Pearce, D. A., Bennett, M. J. and Davidson, B. L. (2000). Batten disease: evaluation of *CLN3* mutations on protein localization and function. *Hum. Mol. Genet.* **9**, 735-744.

Hobert, J. A. and Dawson, G. (2007). A novel role of the Batten disease gene CLN3: association with BMP synthesis. *Biochem. Biophys. Res. Commun.* **358**, 111-116.

Holopainen, J. M., Saarikoski, J., Kinnunen, P. K. and Järvelä, I. (2001). Elevated lysosomal pH in neuronal ceroid lipofuscinoses (NCLs). *Eur. J. Biochem.* **268**, 5851-5856.

Iwaki, T., Osawa, F., Onishi, M., Koga, T., Fujita, Y., Hosomi, A., Tanaka, N., Fukui, Y. and Takegawa, K. (2003). Characterization of *vps33+*, a gene required for vacuolar biogenesis and protein sorting in *Schizosaccharomyces pombe*. *Yeast* **20**, 845-855.

Iwaki, T., Goa, T., Tanaka, N. and Takegawa, K. (2004). Characterization of *Schizosaccharomyces pombe* mutants defective in vacuolar acidification and protein sorting. *Mol. Genet. Genomics* **271**, 197-207.

Iwaki, T., Hosomi, A., Tokudomi, S., Kusunoki, Y., Fujita, Y., Giga-Hama, Y., Tanaka, N. and Takegawa, K. (2006). Vacuolar protein sorting receptor in *Schizosaccharomyces pombe*. *Microbiology* **152**, 1523-1532.

Järvelä, I., Sainio, M., Rantamaki, T., Olkkonen, V. M., Carpén, O., Peltonen, L. and Jalanko, A. (1998). Biosynthesis and intracellular targeting of the CLN3 protein defective in Batten disease. *Hum. Mol. Genet.* **7**, 85-90.

Järvelä, I., Lehtovirta, M., Tikkanen, R., Kyttälä, A. and Jalanko, A. (1999). Defective intracellular transport of CLN3 is the molecular basis of Batten disease (JNCL). *Hum. Mol. Genet.* **8**, 1091-1098.

Junaid, M. A. and Pullarkat, R. K. (1999). Increased brain lysosomal pepstatin-insensitive proteinase activity in patients with neurodegenerative diseases. *Neurosci. Lett.* **264**, 157-160.

Kihara, A., Noda, T., Ishihara, N. and Ohsumi, Y. (2001). Two distinct Vps34 phosphatidylinositol 3-kinase complexes function in autophagy and carboxypeptidase Y sorting in *Saccharomyces cerevisiae*. *J. Cell Biol.* **152**, 519-530.

Kim, Y., Ramirez-Montealegre, D. and Pearce, D. A. (2003). A role in vacuolar arginine transport for yeast Btn1p and for human CLN3, the protein defective in Batten disease. *Proc. Natl. Acad. Sci. USA* **100**, 15458-15462.

Kitaguchi, T., Wisniewski, K. E., Maslinski, S., Maslinska, D., Wisniewski, T. M. and Kim, K. S. (1990). Beta-protein immunoreactivity in brains of patients with neuronal ceroid lipofuscinosis: ultrastructural and biochemical demonstration. *Neurosci. Lett.* **112**, 155-160.

Kitzmüller, C., Haines, R., Codlin, S., Cutler, D. F. and Mole, S. E. (2008). A function retained by the common mutant CLN3 protein is responsible for the late onset of juvenile neuronal ceroid lipofuscinosis (JNCL). *Hum. Mol. Genet.* **17**, 303-312.
Kremmidiotis, G., Lensink, I. L., Bilton, R. L., Woollatt, E., Chataway, T. K., Sutherland, G. R. and Callen, D. F. (1999). The Batten disease gene product (CLN3p) is a Golgi integral membrane protein. *Hum. Mol. Genet.* **8**, 523-531.
Kyttälä, A., Ihrke, G., Vesa, J., Schell, M. J. and Luzio, J. P. (2004). Two motifs target Batten disease protein CLN3 to lysosomes in transfected non-neuronal and neuronal cells. *Mol. Biol. Cell* **15**, 1313-1323.
Lawe, D. C., Patki, V., Heller-Harrison, R., Lambright, D. and Corvera, S. (2000). The FYVE domain of early endosome antigen 1 is required for both phosphatidylinositol 3-phosphate and Rab5 binding. Critical role of this dual interaction for endosomal localization. *J. Biol. Chem.* **275**, 3699-3705.
Lippincott-Schwartz, J., Yuan, L. C., Bonifacino, J. S. and Klausner, R. D. (1989). Rapid redistribution of Golgi proteins into the ER in cells treated with brefeldin A: evidence for membrane cycling from Golgi to ER. *Cell* **56**, 801-813.
Lobley, A., Swindells, M. B., Orengo, C. A. and Jones, D. T. (2007). Inferring function using patterns of native disorder in proteins. *PLoS Comp. Biol*. **3**, e162.
Luiro, K., Kopra, O., Lehtovirta, M. and Jalanko, A. (2001). CLN3 protein is targeted to neuronal synapses but excluded from synaptic vesicles: new clues to Batten disease. *Hum. Mol. Genet.* **10**, 2123-2131.
Luiro, K., Yliannala, K., Ahtiainen, L., Maunu, H., Järvelä, I., Kyttala, A. and Jalanko, A. (2004). Interconnections of CLN3, Hook1 and Rab proteins link Batten disease to defects in the endocytic pathway. *Hum. Mol. Genet.* **13**, 3017-3027.
Metcalf, D. J., Calvi, A. A., Seaman, M. N. J., Mitchison, H. M. and Cutler, D. F. (2008). Loss of the Batten disease gene *CLN3* prevents exit from the TGN of the mannose 6-phosphate receptor. *Traffic* **9**, 1905-1914.
McNiven, M. A. and Thompson, H. M. (2006). Vesicle formation at the plasma membrane and trans-Golgi network: the same but different. *Science* **313**, 1591-1594.
Moreno, S., Klar, A. and Nurse, P. (1991). Molecular genetic analysis of fission yeast *Schizosaccharomyces pombe*. *Methods Enzymol.* **194**, 795-823.
Narayan, S. B., Rakheja, D., Tan, L., Pastor, J. V. and Bennett, M. J. (2006). CLN3P, the Batten's disease protein, is a novel palmitoyl-protein Delta-9 desaturase. *Ann. Neurol.* **60**, 570-577.
Nugent, T., Mole, S. E. and Jones, D. (2008). The transmembrane topology of Batten disease protein CLN3 determined by consensus computational prediction constrained by experimental data. *FEBS Lett.* **582**, 1019-1024.
Osorio, N. S., Carvalho, A., Almeida, A. J., Padilla-Lopez, S., Leao, C., Laranjinha, J., Ludovico, P., Pearce, D. A. and Rodrigues, F. (2007). Nitric oxide signaling is disrupted in the yeast model for Batten disease. *Mol. Biol. Cell* **18**, 2755-2767.
Padilla-Lopez, S. and Pearce, D. A. (2006). *Saccharomyces cerevisiae* lacking Btn1p modulate vacuolar ATPase activity in order to regulate pH imbalance in the vacuole. *J. Biol. Chem.* **281**, 10273-10280.
Patterson, G. H., Hirschberg, K., Polishchuk, R. S., Gerlich, D., Phair, R. D. and Lippincott-Schwartz, J. (2008). Transport through the Golgi apparatus by rapid partitioning within a two-phase membrane system. *Cell* **133**, 1055-1067.
Pearce, D. A. and Sherman, F. (1998). A yeast model for the study of Batten disease. *Proc. Natl. Acad. Sci. USA* **95**, 6915-6918.
Pearce, D. A., Ferea, T., Nosel, S. A., Das, B. and Sherman, F. (1999). Action of *BTN1*, the yeast orthologue of the gene mutated in Batten disease. *Nat. Genet.* **22**, 55-58.
Persaud-Sawin, D. A., VanDongen, A. and Boustany, R. M. (2002). Motifs within the CLN3 protein: modulation of cell growth rates and apoptosis. *Hum. Mol. Genet.* **11**, 2129-2142.
Persaud-Sawin, D. A., Mousallem, T., Wang, C., Zucker, A., Kominami, E. and Boustany, R. M. (2007). Neuronal ceroid lipofuscinosis: a common pathway? *Pediatr. Res.* **61**, 146-152.
Pidoux, A. L. and Armstrong, J. (1993). The BiP protein and the endoplasmic reticulum of *Schizosaccharomyces pombe*: fate of the nuclear envelope during cell division. *J. Cell Sci.* **105**, 1115-1120.
Pohl, S., Mitchison, H. M., Kohlschutter, A., Diggelen, O. V., Braulke, T. and Storch, S. (2007). Increased expression of lysosomal acid phosphatase in CLN3-defective cells and mouse brain tissue. *J. Neurochem.* **103**, 2177-2188.
Ramirez-Montealegre, D. and Pearce, D. A. (2005). Defective lysosomal arginine transport in juvenile Batten disease. *Hum. Mol. Genet.* **14**, 3759-3773.
Ridley, S. H., Ktistakis, N., Davidson, K., Anderson, K. E., Manifava, M., Ellson, C. D., Lipp, P., Bootman, M., Coadwell, J., Nazarian, A. et al. (2001). FENS-1 and DFCP1 are FYVE domain-containing proteins with distinct functions in the endosomal and Golgi compartments. *J. Cell Sci.* **114**, 3991-4000.
Robinson, J. S., Klionsky, D. J., Banta, L. M. and Emr, S. D. (1988). Protein sorting in *Saccharomyces cerevisiae*: isolation of mutants defective in the delivery and processing of multiple vacuolar hydrolases. *Mol. Cell. Biol.* **8**, 4936-4948.
Rothman, J. H. and Stevens, T. H. (1986). Protein sorting in yeast: mutants defective in vacuole biogenesis mislocalize vacuolar proteins into the late secretory pathway. *Cell* **47**, 1041-1051.
Schaub, B. E., Berger, B., Berger, E. G. and Rohrer, J. (2006). Transition of galactosyltransferase 1 from trans-Golgi cisterna to the trans-Golgi network is signal mediated. *Mol. Biol. Cell* **17**, 5153-5162.
Siintola, E., Lehesjoki, A. E. and Mole, S. E. (2006). Molecular genetics of the NCLs-status and perspectives. *Biochim. Biophys. Acta* **1762**, 857-864.
Siintola, E., Topcu, M., Aula, N., Lohi, H., Minassian, B. A., Paterson, A. M., Liu, X.-Q., Wilson, C., Lahtinen, U., Anottonen, A.-K. et al. (2007). The novel neuronal ceroid lipofusinosis gene MFSD8 encodes a putative lysosomal transporter. *Am. J. Hum. Genet.* **81**, 136-146.
Sleat, D. E., Sohar, I., Pullarkat, P. S., Lobel, P. and Pullarkat, R. K. (1998). Specific alterations in levels of mannose 6-phosphorylated glycoproteins in different neuronal ceroid lipofuscinoses. *Biochem. J.* **334**, 547-551.
Stack, J. H., DeWald, D. B., Takegawa, K. and Emr, S. D. (1995). Vesicle-mediated protein transport: regulatory interactions between the Vps15 protein kinase and the Vps34 PtdIns 3-kinase essential for protein sorting to the vacuole in yeast. *J. Cell Biol.* **129**, 321-334.
Storch, S., Pohl, S., Quitsch, A., Falley, K. and Braulke, T. (2007). C-terminal prenylation of the CLN3 membrane glycoprotein is required for efficient endosomal sorting to lysosomes. *Traffic* **8**, 431-444.
Tabuchi, M., Iwaihara, O., Ohtani, Y., Ohuchi, N., Sakurai, J., Morita, T., Iwahara, S. and Takegawa, K. (1997). Vacuolar protein sorting in fission yeast: cloning, biosynthesis, transport, and processing of carboxypeptidase Y from *Schizosaccharomyces pombe*. *J. Bacteriol.* **179**, 4179-4189.
Takegawa, K., DeWald, D. B. and Emr, S. D. (1995). *Schizosaccharomyces pombe* Vps34p, a phosphatidylinositol-specific PI 3-kinase essential for normal cell growth and vacuole morphology. *J. Cell Sci.* **108**, 3745-3756.
Tanaka, N. and Takegawa, K. (2001). Functional characterization of Gms1p/UDP-galactose transporter in *Schizosaccharomyces pombe*. *Yeast* **18**, 745-757.
Valls, L. A., Winther, J. R. and Stevens, T. H. (1990). Yeast carboxypeptidase Y vacuolar targeting signal is defined by four propeptide amino acids. *J. Cell Biol.* **111**, 361-368.
Villanova, M., Ceuterick, C., Dotti, M. T., Santorelli, F. M., Casali, C., Malandrini, A., De Stefano, N., Lubke, U., Martin, J. J., Guazzi, G. C. et al. (1999). Detection of beta-A4 amyloid and its precursor protein in the muscle of a patient with juvenile neuronal ceroid lipofuscinosis (Spielmeyer-Vogt-Sjogren). *Acta Neuropathol.* **98**, 78-84.
Vjestica, A., Tang, X. Z. and Oliferenko, S. (2008). The actomyosin ring recruits early secretory compartments to the division site in fission yeast. *Mol. Biol. Cell* **19**, 1125-1138.
Whyte, J. R. and Munro, S. (2001). A yeast homolog of the mammalian mannose 6-phosphate receptors contributes to the sorting of vacuolar hydrolases. *Curr. Biol.* **11**, 1074-1078.
Wisniewski, K. E., Maslinska, D., Kitaguchi, T., Kim, K. S., Goebel, H. H. and Haltia, M. (1990). Topographic heterogeneity of amyloid B-protein epitopes in brains with various forms of neuronal ceroid lipofuscinoses suggesting defective processing of amyloid precursor protein. *Acta Neuropathol.* **80**, 26-34.
Wisniewski, K. E., Gordon-Majszak, W., Maslinski, S. and Heaney-Kieras, J. (1992). Altered protein patterns in brains of children with neuronal ceroid lipofuscinosis. *Am. J. Med. Genet.* **42**, 568-574.
Wurmser, A. E. and Emr, S. D. (2002). Novel PtdIns(3)P-binding protein Etf1 functions as an effector of the Vps34 PtdIns 3-kinase in autophagy. *J. Cell Biol.* **158**, 761-772.
Yan, Y. and Backer, J. M. (2007). Regulation of class III (Vps34) PI3Ks. *Biochem. Soc. Trans.* **35**, 239-241.
Zeng, X., Overmeyer, J. H. and Maltese, W. A. (2006). Functional specificity of the mammalian Beclin-Vps34 PI 3-kinase complex in macroautophagy versus endocytosis and lysosomal enzyme trafficking. *J. Cell Sci.* **119**, 259-270.

Supplementary Table I Strains

Strain	Genotype	Source
972	*h⁻*	Laboratory stock
Wild-type (wt)	*ura4-D18, leu1-32*	Laboratory stock
ED665	*h⁻, ura4-D18, leu1-32, his2*	Laboratory stock
YG660 *(btn1Δ)*	*h⁺, btn1::leu2, ura4-D18, leu1-32, his2*	Laboratory stock
SC1D *(btn1Δ)*	*h⁻, btn1::leu2, leu1-32*	Laboratory stock
SC3D *(btn1Δ)*	*h⁺, btn1::ura4, ura4-D18, leu1-32*	Laboratory stock
SC259A (ED665 + pREP41GFP)	*h⁻, ura4-D18, leu1-32, his2*	Laboratory stock
SC261A (ED665 + pREP41GFP-Btn1p)	*h⁻, ura4-D18, leu1-32, his2*	Laboratory stock
SC585D (ED665 + pREP41GFP-Btn1p^{G136A})	*h⁻, ura4-D18, leu1-32, his2*	Laboratory stock
SC267A (SC3D + pREP41GFP)	*h⁺, btn1::ura4, ura4-D18, leu1-32*	This study
SC269A (SC3D + pREP41GFP-Btn1p)	*h⁺, btn1::ura4, ura4-D18, leu1-32*	This study
SC271A (SC3D + pREP41GFP- Btn1p^{G136A})	*h⁺, btn1::ura4, ura4-D18, leu1-32*	This study
SC2A (YG660 + pREP42GFP	*h⁺, btn1::leu2, ura4-D18, leu1-32, his2*	Laboratory stock
SC5A (YG660 + pREP42GFP-Btn1p	*h⁺, btn1::leu2, ura4-D18, leu1-32, his2*	Laboratory stock
SC522D (YG660 + pREP42GFP-CLN3p	*h⁺, btn1::leu2, ura4-D18, leu1-32, his2*	Laboratory stock
SC580D (wt + pAL-nmt41p-vps10-YFP)	*h⁻, ura4-D18, leu1-32*	This study
SC14F (wt + pAU-gms1-CFP)	*h⁻, ura4-D18, leu1-32*	This study
SC22F (wt + pAU-gms1-CFP +pREP41GFP)	*h⁻, ura4-D18, leu1-32*	This study
SC19F (wt + pAU-gms1-CFP +pREP41GFP-Btn1p)	*h⁻, ura4-D18, leu1-32*	This study
SC27F (wt + pAU-gms1-CFP +pREP41GFP-Btn1p^{G136A})	*h⁻, ura4-D18, leu1-32*	This study
SC28F (wt + pAU-gms1-CFP +pAL-nmt41p-vps10-YFP)	*h⁻, ura4-D18, leu1-32*	This study
SC16F (YG660 + pAU-gms1-CFP)	*h⁺, btn1::leu2, ura4-D18, leu1-32, his2*	This study
SC557D (SC3D + pAL-nmt41p-vps10-YFP)	*h⁺, btn1::ura4, ura4-D18, leu1-32*	This study
cpy1Δ	*h⁺, cpy1::ura4, ura4-D18, leu1-32, his2, ade6-M216*	K. Takegawa (Iwaki et al., 2006, Tabuchi et al., 1997)
vps26Δ	*h⁻, vps26::ura4, ura4-D18, leu1-32*	K. Takegawa (Iwaki et al., 2006)
SC12F (*vps26Δ* + pAL-nmt41p-vps10-YFP)	*h⁻, vps26::ura4, ura4-D18, leu1-32*	This study
SC52F (*vps26Δbtn1Δ*)	*H, vps26::ura4, btn1::leu2, ura4-D18, leu1-32*	This study
vps10Δ	*h⁹⁰, vps10::ura4, ura4-D18, leu1-32*	K. Takegawa (Iwaki et al., 2006)
SC53F (*vps10Δ btn1Δ*)	*H, vps10::ura4, btn1::leu,2 ura4-D18, leu1-32, his2*	This study
vps34Δ	*h⁻, vps34::ura4, ura4-D18, leu1-32, ade6-M216*	K. Takegawa (Iwaki et al., 2006, Takegawa et al,. 1995)
SC9D (*vps34Δbtn1Δ*)	*H, vps34::ura4, btn1::leu2, ura4-D18, leu1-32, ade6-M216, his2*	This study
SC618D (*vps26Δ* + pREP41GFP)	*h⁻, vps26::ura4, ura4-D18, leu1-32*	This study
SC556D (*vps26Δ* + pREP41GFP-Btn1p)	*h⁻, vps26::ura4, ura4-D18, leu1-32*	This study
SC611D (*vps10Δ* + pREP41GFP)	*h⁹⁰, vps10::ura4, ura4-D18, leu1-32*	This study
SC614D (*vps10Δ* + pREP41GFP-Btn1p)	*h⁹⁰, vps10::ura4, ura4-D18, leu1-32*	This study
SC500A (*vps34Δ* + pREP41GFP)	*h⁻, vps34::ura4, ura4-D18, leu1-32, ade6-M216*	This study
SC502A (*vps34Δ* + pREP41GFP-Btn1p)	*h⁻, vps34::ura4, ura4-D18, leu1-32, ade6-M216*	This study
SC505A (*vps34Δ* + pREP41GFP-Btn1p^{G136A})	*h⁻, vps34::ura4, ura4-D18, leu1-32, ade6-M216*	This study
SO1511 (Anp1p-GFP)	*h⁺, anp1-GFP::ura4, ura4-D18, leu1-32, ade6-M216*	S. Oliferenko (Vjestica et al., 2008)
MBY671 (Ost1p-GFP)	*h⁻, ost1-GFP::ura4, ura4-D18, leu1-32*	S. Oliferenko (Vjestica et al., 2008)